Towards More Possibilities: Motion Planning and Control for Hybrid Locomotion of Wheeled-legged Robots

Jingyuan Sun[1*], Yangwei You[2*], Xuran Zhao[1], Albertus Hendrawan Adiwahono[2], Chee Meng Chew[1]

***Abstract*—This paper proposed a control framework to tackle the hybrid locomotion problem of wheeled-legged robots. It comes as a hierarchical structure with three layers: hybrid foot placement planning, Centre of Mass (CoM) trajectory optimization and whole-body control. General mathematical representation of foot movement is developed to analyze different motion modes and decide hybrid foot placements. Gait graph widely used in legged locomotion is extended to better describe the hybrid movement by adding extra foot velocity information. Thereafter, model predictive control is introduced to optimize the CoM trajectory based on the planned foot placements considering terrain height changing. The desired trajectories together with other kinematic and dynamic constraints are fed into a whole-body controller to produce joint commands. In the end, the feasibility of the proposed approach is demonstrated by the simulation and experiments of hybrid locomotion running on our wheeled quadrupedal robot Pholus.**

***Index Terms*—Legged Robots, Natural Machine Motion, Climbing Robots**

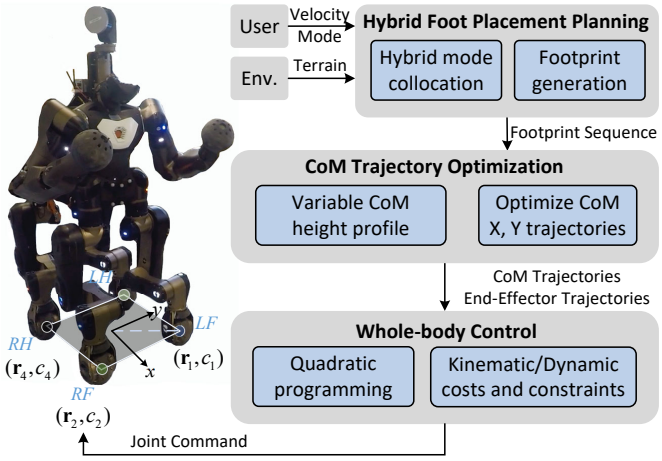

Fig. 1. Wheeled-legged robot Pholus with the proposed control framework. In the model, $\mathbf{r}_i$ stands for the position of foot i, c_i represents the corresponding contact status, and $i = 1, 2, 3, 4$ indicates the left front(LF), right front(RF), left hind (LH) and right hind(RH) leg respectively.

I. Introduction

INSPIRED by the high versatility and adaptability of animals on rough terrains, a lot of research has been done to develop legged robots which are expected to walk and run in a natural environment [1]–[5]. On the other hand, myriad vehicles with wheels have been existing and evolving for hundreds of years due to its high energy efficiency and easy-to-build. How to incorporate the best properties of the two disparate mobile systems into one hybrid platform has long been a hot topic in robotics research, which promises more possibilities to explore various terrains safely and efficiently. To address this problem, this paper contributed to the motion planning and control for the hybrid locomotion of wheeled-legged robots.

The control of wheeled robots has been widely and deeply studied [6], [7], and many research results have been successfully applied to commercial robots, like autonomous vehicle, vacuum cleaner robot, and driverless forklift. Some classic control algorithms have also been open-sourced and widely adopted among the robotic community. On the contrary, legged locomotion has long been a challenging problem owing to its system complexity of high degrees of freedom (DoF) and sensitivity to the movement stability. Recently, together with the advance of torque-controlled actuators, legged robots have witnessed significant improvement in the performance of dynamic movement. Among these impressive robots, most of the control approaches fall into three categories: heuristic methods by adjusting foot placements [1], [8], bio-inspired CPG control strategies [9] and optimization-based model predictive control [10], [11]. As a combination of these two mobile types, hybrid locomotion of wheeled-legged robots which we discussed in this paper is based on the remarkable work of these two research areas.

A. Related Work

Due to motion flexibility and efficiency, hybrid systems with a combination of legs and wheels have become popular in recent years. Some wheeled-legged platforms implemented control frameworks based on kinematic analysis [12], [13], while some researchers relied on dynamics modelling to generate joint torque commands for either the upper body or the whole body force control [14], [15]. However, most of these works have not exploited the mobility of the legs and

Manuscript received: September, 10, 2019; Revised December, 17, 2019; Accepted January, 18, 2020.

This paper was recommended for publication by Editor Nikos Tsagarakis upon evaluation of the Associate Editor and Reviewers' comments.

*These authors contributed equally to this work.

[1]Department of Mechanical Engineering, National University of Singapore, 117575, Singapore, j.sun@u.nus.edu

[2]Institute for Infocomm Research, Agency for Science, Technology and Research, 138632, Singapore, youy@i2r.a-star.edu.sg

Digital Object Identifier (DOI): see top of this page.

only treated the robot as a mobile robot. In other words, they don't really use the legs for locomotion.

In contrast, some robots in the DARPA Robotics Challenge (DRC) have two mobility modes to choose: walking mode to traverse challenging terrain and wheel mode to fast roll on flat ground. The DRC winner robot DRC-HUBO+ [16] has a humanoid body with two wheels attached to the knees. This structure allows the robot to switch between the walking mode and wheel mode by altering the posture of its legs. In the wheel mode, the robot needs to knee on the ground which tremendously restricts the contribution of legs to mobility.

RoboSimian [17], a quadrupedal robot with two active wheels on its body and two caster wheels on its limbs, allows driving motions on even terrain. During driving, the robot only relies on the wheels while the legs are in a crouched position and not used.

Unlike DRC-HUBO+ and RoboSimian, Momaro [18], a dual-arm quadrupedal robot, has an active-controlled wheel under each of its feet, which means it doesn't need to transform to a specific pose to stay in the driving mode. Moreover, omni-directional driving comes out as a bonus thanks to its high DOFs legs. As a descendant of Momaro, Centauro [11] has one more hip yaw joint to further enhance legs' manipulability. A driving-stepping strategy has been successfully demonstrated on both Momaro and Centauro robots to allow traversing stairs [19], [20]. This strategy works quite well in this specific scenario though not general and systematic enough to cover more use cases.

Researchers from ETH [21] installed additional wheels at the end of legs of their robot ANYmal. All the joints are fully torque-controlled including the wheels. Based on this, they developed several control algorithms to achieve hybrid locomotion. For instance, [22] presented a hierarchical control framework which adopts the trajectory optimization method and elaborates the kinematic rolling constraint of wheels. And [21] proposed another trajectory optimizer which can run online at 50Hz with linearized Zero Moment Point (ZMP) constraints.

Another interesting work from the computer graphics group showed a general computation-driven approach to design optimization and motion synthesis for robots having arbitrary arrangements of legs and wheels. This can be a promising direction to explore in the future while more concern needs to be taken on the heavy computation load [23].

B. Contribution

Compared with existing work on hybrid locomotion, we endeavour to develop an effective yet light-weight hybrid locomotion framework, general and flexible enough to address miscellaneous motion modes of wheeled-legged robots. The main contributions of this paper are listed below:

1) General mathematical representation and extended gait graphs were proposed to help analysis of hybrid locomotion. And hybrid foot placement planning of typical use cases was fully introduced to stress the advantages of hybrid locomotion.
2) Model predictive control (MPC) was implemented for Center of Mass (CoM) trajectory optimization under hybrid foot placements, different from the discrete ones of pure legged locomotion. In addition, variable CoM height is considered to handle uneven terrains.
3) Hierarchical control structure combining with light-weight whole-body IK solver enables the whole controller to run online at 200Hz on our dual-arm quadrupedal robot Pholus. (see Fig. 1).

This paper is organized as follows. In Section II, hybrid foot placement planning and CoM trajectory optimization are introduced as the core of motion planning. Then, Section III presents the optimization-based whole-body controller. And the proposed control approach is evaluated through simulation and experiments in Section IV. The paper ends with conclusions and an outlook on future research.

II. Motion Planning

Following classic control structures of legged locomotion, our framework is comprised of several layers to simplify the whole control problem as shown in Fig. 1. Robots first take terrain information from perception module and control commands from users and then plan foot placements according to different motion modes of hybrid wheeled-legged locomotion. Thereafter, based on planned foot sequences, CoM trajectories along forward and lateral directions can be optimized given a terrain-decided CoM height profile. At the bottom of this control framework, a whole-body controller is implemented to determine optimal joint commands considering different kinematic and dynamical costs and constraints via quadratic programming. In this section, we will focus on the motion planning part which includes the hybrid foot placement planning module and the CoM optimization module. And the whole-body controller will be introduced next.

A. Hybrid Foot Placement Planning

To describe the foot movement of wheeled-legged robots, we can use a tuple for each leg:

$$(\mathbf{r}_i, c_i), i \in F = \{1, 2, 3 \cdots n\} \tag{1}$$

where n is the total number of legs (for example, 4 for our quadrupedal robot, 2 for bipedal and 6 for hexapodal), i stands for one specific leg, $\mathbf{r}$ is the foot position, and c represents the contact status: 1 for supporting on the ground, 0 for swinging in the air.

$(\mathbf{r}_i, c_i)$ is a general and flexible representation of the foot movement in hybrid wheeled-legged locomotion. To be realistic, some physical constraints are usually held:

$$\underline{L}_{ij} < \|\mathbf{r}_i - \mathbf{r}_j\|_2 < \overline{L}_{ij}, \forall i, j \in F, i \neq j \tag{2}$$

$$c_i = 1 \Rightarrow \mathbf{r}_i \in G, \forall i \in F \tag{3}$$

where Eq. (2) considers about simplified kinematic constraints exerting on robots that two feet cannot reach to each other too far or too close, and Eq. (3) implies that feet of supporting legs should stay on the ground surface G. These two constraints are always held for the foot placement planning of hybrid wheeled-legged locomotion. Coming with the complexity and high DoFs of wheeled-legged robots, the possible movement

form can be infinite if only given the two constraints. Therefore, some specific motion modes are defined to allow for intuitive control.

1) Driving mode: In favour of its energy efficiency, driving mode is very commonly used on flat ground. In this mode, the robot will not take steps to walk forward, instead, it always rolls. A typical omni-directional driving motion with all the feet on the ground can be defined as following [24]:

$$\dot{\mathbf{r}}_i = \dot{\mathbf{r}}_0 + \omega \times \mathbf{l}_i + \dot{\mathbf{l}}_i, c_i = 1, \forall i \in F \tag{4}$$

where $\dot{\mathbf{r}}_0$ and ω are individually the linear and angular velocities of virtual centre representing the overall movement of the robot, and $\mathbf{l}_i$ is the current position of foot i with respect to the virtual centre. Velocity $\dot{\mathbf{l}}_i$ indicates possible simultaneous leg movement while driving. This functionality can be quite useful if we need robots to transform while driving. Considering the nonholonomic rolling constraint, wheel's spinning direction should be steered to keep aligned with the desired velocity of each foot [22]. This constraint should also be taken into account for other motion modes whenever wheels are rolling.

Gait graph is a popular and straightforward tool for scheduling contact status of different gaits, therefore here we extend it by adding desired velocity information of each foot to better describe hybrid locomotion. For instance, when our wheeled quadrupedal robot Pholus is driving forward with a constant velocity, its gait graph can be depicted as Fig. 2 a), where the dark blue means all the feet are on the ground and the yellow line indicates the forward velocity of each foot.

2) Walking mode: Walking has been thoroughly studied on legged robots for traversing rough terrain. Inspired by animals' movement, various gaits haven been proposed as spatio-temporal patterns. Though gaits can be very different from each other, they share some key characteristics such as periodicity and stationary feet of supporting legs:

$$\begin{aligned} \dot{\mathbf{r}}_i(t) &= \dot{\mathbf{r}}_i(t-T), \forall i \in F \\ c_i(t) = 1 &\Rightarrow \dot{\mathbf{r}}_i(t) = 0, \forall i \in F \end{aligned} \tag{5}$$

where t is the current time and T is the duration of one gait phase including swinging time T_{sw} and supporting time T_{st}. Another distinct feature of walking mode is the status switch of one leg between support and swing. Fig. 2 b) shows a typical walking gait with a leg lift-up sequence: left front → right hind → right front → left hind. In this case, the foot movements can be defined as:

$$\mathbf{r}_i(t) = \begin{cases} \mathbf{r}_0(t_i^{td}) + \mathbf{R}(\theta(t_i^{td}))\mathbf{L}_i, c_i(t) = 1 \\ (1-k)\cdot \mathbf{r}_i(t_i^{td}) + k \cdot \mathbf{r}_i(t_i^{td} + T), c_i(t) = 0 \end{cases} \tag{6}$$

where t_i^{td} is the latest touch-down time of leg i, $\mathbf{R}$ is the rotation matrix, θ is the rotation angle of virtual centre as defined above for ω, $\mathbf{L}_i$ is the fixed foot position with respect to the virtual center defined for this gait, and $k = (t - t_i^{td})/T_{sw}$ is the time percentage within a swing phase.

3) Hybrid mode: As a combination of driving mode and walking mode, hybrid mode targets at taking advantage of the best from the two worlds. Instead of always keeping all the feet on the ground like in the driving mode, the robot is also able to lift its legs to handle unstructured environments which can significantly increase its maneuverability and adaptability. Besides, without restricting the foot velocities of supporting legs to be zero, hybrid mode promises high energy efficiency and movement speed. Although hybrid mode is a very miscellaneous functionality, here we will only address two of its useful and interesting cases: obstacle crossing and moonwalk.

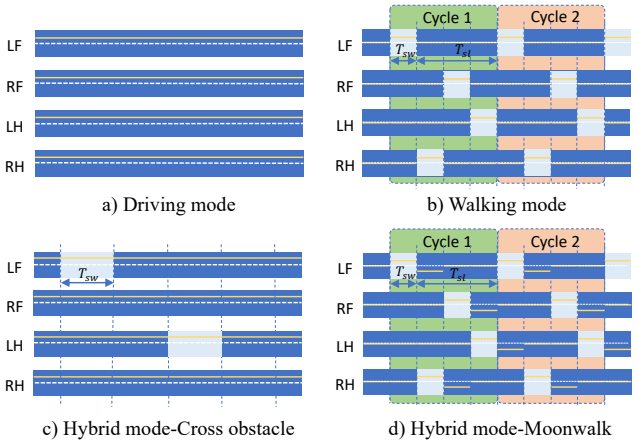

Fig. 2. The gait graphs of different motion modes. The dark blue color represents the supporting phase and the light blue color stands for the swinging phase. The yellow solid line shows the foot forward velocity. And the white dashed line indicates the neutral zero velocity.

Obstacle crossing of hybrid mode is a valuable capability which allows robots to drive over obstacles by lifting its legs without stopping or making a detour. Its gait graph can be very similar to driving mode's. Fig. 2 c) is an example when the robot drives across a thin obstacle plane on the left side. The key problem of obstacle crossing is to determine when and which leg should be lifted according to the obstacle size and the desired moving velocity. Given the obstacle pose and shape, the desired velocities of virtual center $[\dot{\mathbf{r}}_0 \ \omega]^T$ and predefined foot configuration $\mathbf{L}_i$ of each leg like for the walking mode, preliminary foot prints can be generated following the driving mode according to Eq. (3) and (4). After this, two more things should be concerned. One is to smooth the height change of foot prints considering the possible discontinuity of terrain when obstacle exists. The other is to decide the contact status c_i and the corresponding ground clearness.

Take a quadrupedal robot as an example. As shown in Fig. 3, the robot tries to drive across a thin obstacle plane. When one foot i reaches a distance $\mathbf{d_i}$ away from the obstacle, it will be lifted up to allow for enough time to achieve a smooth transition to the height of obstacle. The distance $\mathbf{d_i}$ should satisfy:

$$\mathbf{d}_i > \int_{t_i^{top} - T_{lf}}^{t_i^{top}} (\dot{\mathbf{r}}_0 + \omega \times \mathbf{L}_i) dt, \ T_{lf} = \frac{\Delta H}{\dot{r}_{max}^z} \tag{7}$$

where t_i^{top} is the time when the foot i reaches the top of the obstacle, ΔH is the resulting lift height and $\dot{r}_{max}^z$ is the maximum velocity of foot movement along vertical direction decided by the robot hardware. This kind of constraint also exists when the leg gets off the obstacle.

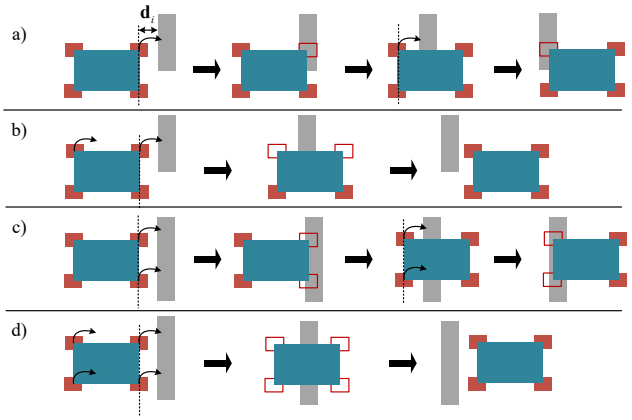

Fig. 3. Four different scenarios of crossing an obstacle. The red hollow rectangle means one leg in swing phase, and the filled red rectangle indicates one leg in support phase. a) LF and LH legs swing one after another. b) The swing phases of LF and LH legs overlap similar to pace gait. c) The hind leg pairs swing after the front leg pairs similar to bounding gait. d) All the four legs swing together like jumping.

Fig. 4. Obstacle size determines whether the feet need to step on the obstacle. For long obstacles, better to step on to increase movement stability.

When crossing obstacles, different gaits can be observed depending on how many legs are lifted up simultaneously. In Fig. 3, plot a) shows the case where the robot lifts up LF and LH legs one by one without overlapping swing phase between the two. However, if moving fast enough, there could be a period when both LF and LH legs are swinging in the air which looks like the pace gait as shown in plot b). Plot c) and d) shows similar consideration but the width of obstacle is longer and blocks both the left and right sides resulting bounding-like and jumping-like gaits. Generally speaking, the foot movements of obstacle crossing can be written as:

$$\begin{gathered}\dot{\mathbf{r}}_i^{x,y} = \dot{\mathbf{r}}_0^{x,y} + (\omega \times \mathbf{L}_i)^{x,y}, \forall i \in F \\ \begin{cases} \dot{\mathbf{r}}_i^z = f(t), c_i(t) = 0, \ t \in (t_i^{top} - T_{lf}, t_i^{top} + T_{lf}) \\ \dot{\mathbf{r}}_i^z = \dot{\mathbf{r}}_0^z + (\omega \times \mathbf{L}_i)^z, c_i(t) = 1, \ otherwise \end{cases}\end{gathered} \tag{8}$$

where the superscripts x, y, z indicate the motion coordinate, and $f(t)$ is a motion profile function of swing legs along the vertical direction which is usually a customized polynomial trajectory. Different $f(t)$ will not affect the subsequent CoM optimization because the corresponding leg is swinging. Obviously, the main difference between the driving Eq. (4) and the hybrid obstacle crossing Eq. (8) happens in the z direction.

In addition, the size of obstacles will also affect the contact status of lifting legs. As shown in Fig. 4, the robot lifts up its LF foot after encountering an obstacle. Since the obstacle is so long, the LH leg also needs to be lifted up before the LF leg touches down. In this case, instead of forcing the robot to drive with only two right wheels, it is better to allow LF and LH feet touching on the obstacle to enlarge the support polygon and improve the stability.

Another interesting show case of hybrid mode is moonwalk where the legs swing forward first after lifting up and then roll back as depicted in Fig. 2 d). It creates a visual illusion that the robot looks as if it is walking forward but actually stays in place as long as the equation $\int_t^{t+T} \dot{\mathbf{r}}_i dt = 0$ holds. One of the straightforward solutions is the one shown in the gait graph and demonstrated in the following experiment, and its foot movements are quite similar to the walking mode as below:

$$\begin{gathered}\mathbf{r}_i(t) = \begin{cases} (1 - k^{td}) \cdot \mathbf{r}_i(t_i^{td}) + k^{td} \cdot \mathbf{r}_i(t_i^{lf}), c_i(t) = 1 \\ (1 - k^{lf}) \cdot \mathbf{r}_i(t_i^{lf}) + k^{lf} \cdot \mathbf{r}_i(t_i^{td}), c_i(t) = 0 \end{cases} \\ k^{lf} = \frac{t - t_i^{lf}}{T_{sw}}, k^{td} = min(\frac{t - t_i^{td}}{T_{sw}}, 1)\end{gathered} \tag{9}$$

where t_i^{td} and t_i^{lf} are individually the latest touch-down and lift-up time of leg i. And the leg lift-up sequence is also: left front $\rightarrow$ right hind $\rightarrow$ right front $\rightarrow$ left hind.

B. CoM Trajectory Optimization

Given planned foot prints and corresponding contact status, we can optimize CoM trajectory considering movement stability and trajectory smoothness. Recently, MPC has become very popular to address this problem in the research community of legged robots due to its conciseness and flexibility [4], [10], [25]. This paper also adopts this approach by discretizing hybrid foot placements with equal interval time, like 0.1s used in the following experiments. And a centroidal model is taken to describe the overall robot dynamics without considering detailed joint configurations:

$$C_{x,y} - \frac{mC_z\ddot{C}_{x,y} - \dot{L}_{y,x}}{m(\ddot{C}_z + g)} = Z_{x,y} \in conv\{\mathbf{r}_i\} \tag{10}$$

where C stands for the motion of CoM and Z for ZMP, m is the total mass of the robot, L is the angular momentum around CoM, g is the gravitational acceleration constant and $conv\{\mathbf{r}_i\}$ represents the convex hull of foot prints. Those subscripts indicate the motion coordinate.

How to deal with angular momentum L is still an open question in legged locomotion, thus here we will ignore it as well [26]. To consider CoM height changing on uneven terrain without breaking model linearity, we can define the height trajectory beforehand so that C_z and $\ddot{C}_z$ are known. In this case, the centroidal model can be simplified as:

$$C_{x,y} - \frac{C_z}{\ddot{C}_z + g}\ddot{C}_{x,y} = C_{x,y} - K\ddot{C}_{x,y} = Z_{x,y} \in conv\{\mathbf{r}_i\} \tag{11}$$

where $\frac{C_z}{\ddot{C}_z + g}$ can be treated as a predefined parameter K.

Besides, the motion equation of CoM can be discretized as:

$$\begin{gathered}\mathbf{X}_{x,y}^{k+1} = \mathbf{A}\mathbf{X}_{x,y}^k + \mathbf{B}\dddot{C}_{x,y}^k \\ \mathbf{A} = \begin{bmatrix} 1 & dt & \frac{dt^2}{2} \\ 0 & 1 & dt \\ 0 & 0 & 1 \end{bmatrix}, \mathbf{B} = \begin{bmatrix} \frac{dt^3}{6} \\ \frac{dt^2}{2} \\ dt \end{bmatrix}, \mathbf{X} = \begin{bmatrix} C \\ \dot{C} \\ \ddot{C} \end{bmatrix}\end{gathered} \tag{12}$$

where superscript k is the knot number of discretization, and dt is the duration between two knots.

Based on Eq. (11) and (12), an optimization problem can be formulated to calculate the CoM trajecotry following the MPC paradigm:

$$\min_{\dddot{\mathbf{C}}^{k}_{x,y}} \quad \alpha||\dddot{\mathbf{C}}^{k}_{x,y}||^2 + \beta||\mathbf{Z}^{k+1}_{x,y} - {}^{ref}\mathbf{Z}^{k+1}_{x,y}||^2 \tag{13}$$

where the CoM jerks $\dddot{\mathbf{C}}^{k}_{x,y}$ is the decision variable, and ${}^{ref}\mathbf{Z}^{k+1}_{x,y}$ is the ZMP references lying in the center of support polygon decided by the planned foot placements. In order to take the future states into consideration, the CoM and ZMP variables are vectors containing the current knot and future knots within a fix-size time window. The cost function of this optimization problem is to minimize the CoM jerk and the ZMP deviation from the center of support polygon. The CoM jerk affects the smoothness of the trajectory. Smaller jerk means a smoother trajectory. And the ZMP deviation indicates the stability of movement. The bigger the deviation is, the smaller the stability margin is. α and β are the weights to balance between the two criteria. Although the second item of cost function can work as a soft constraint to attract ZMP to the centre, a hard constraint to restrict ZMP within support polygon is still necessary for more dynamic motions like troting and bounding. How to formulate a linearized ZMP constraint for hybrid locomotion can refer to [21].

III. Whole-body Control

Hybrid wheeled-legged locomotion is a complicated multi-task motion involving whole-body kinematics and dynamics. Apart from the trajectory tracking of end-effectors in Cartesian space, it also involves body posture regulation, self-collision avoidance and balancing maintenance, etc. Traditional null-space projection-based techniques have been applied to address multi-task problems in a hierarchical manner before [27], [28]. However, these analytical techniques can not properly handle inequality constraints, such as joint limits and friction cone. That is why nowadays more and more researchers turn to numerical optimization methods which permit more flexibility when constructing cost functions and constraints. Although implementation details differ, most of the approaches treat the floating-base inverse kinematics (IK) or inverse dynamics (ID) as a quadratic programming (QP) problem with equality and inequality constraints [22], [29], [30]. Similarly, we formulated the whole-body controller as a QP problem based on the robotic optimization framework OpenSot [31]:

$$\begin{aligned} \min_{\mathbf{X}} \sum_{i=1}^{n} \frac{\omega_i}{2} \|\mathbf{A}_\mathrm{i}\mathbf{X} - \mathbf{b}_\mathrm{i}\|^2 \\ s.t.\ \mathbf{A}_{eq}\mathbf{X} = \mathbf{b}_{eq} \\ \underline{\mathbf{c}} \leqslant \mathbf{C}\mathbf{X} \leqslant \overline{\mathbf{c}} \end{aligned} \tag{14}$$

where the decision variable $\mathbf{X}$ is joint velocities $\dot{\mathbf{q}}$, $\|\mathbf{A}_\mathrm{i}\mathbf{X} - \mathbf{b}_\mathrm{i}\|^2$ are the cost functions to be minimized, $\mathbf{A}_{eq}\mathbf{X} = \mathbf{b}_{eq}$ and $\underline{\mathbf{c}} \leqslant \mathbf{C}\mathbf{X} \leqslant \overline{\mathbf{c}}$ are the equality and inequality constraints, respectively. Due to the difficulty on hardware to achieve joint torque control and also to keep the whole controller computation-light, we formulated the whole-body control as a numerical IK problem. Different weights ω_i are assigned to balance multiple tasks in the cost function without considering strict priorities among them, which is simple to implement and also numerically robust. Hard constraints such as joint limits are defined as inequality constraints. All the objectives and constraints used by the whole-body controller are listed in TABLE I.

TABLE I
Cost functions and constraints of the optimization problem for the whole-body control.

Type	Task	ω	Purpose
Objective	CoM tracking	1	Track the reference CoM trajectory
Objective	Foot tracking	1	Track the reference foot trajectories
Objective	Regulate pelvis	1	Keep the desired orientation of pelvis
Objective	Maintain upper body posture	0.1	Hold the desired joint position of upper body including the torso, dual arms and neck
Objective	Minimize joint velocity	0.1	Smooth the motion and relieve the IK singularity issue
Constraint	Joint limit	N.A.	Avoid hitting the joint position limits

Among the five objective functions listed in the table, the tasks of CoM tracking, foot tracking and pelvis regulation are assigned higher weights since they are considered more important than others. They stand for the execution of the planning results from motion planning module introduced in Section II. On the contrary, maintaining the posture of upper body and minimizing the joint velocities are not that imperative and can be compromised for other more important tasks. For instance, when the robot is walking, instead of always holding at the homing position, the torso can be observed rotating left and right to assist the shifting of CoM. This is also the amazing part of whole-body control being able to coordinate all the joints and balance among multiple tasks. Regarding hybrid locomotion, nonholonomic rolling constraints are specially addressed to ensure that wheel' spinning direction is consistent with the desired velocity of each foot.

IV. Simulation & Experiment

To validate the eligibility of the proposed hybrid control framework and show the potential advantages of wheeled-legged robots, we carried out three experiments and one simulation on a dual-arm wheeled-legged quadrupedal robot Pholus. Overall, the robot possesses 41 DoFs (six for each leg including the rotating wheel joint) and weighs 92 kg. The robot has a width along the shoulders of 61 cm and also an overall pelvis length of 61 cm. In full squat, its height is 112 cm while with fully extended legs its height increases to 171 cm. More details about this robot can be found in [5].

Simulation and experiments were introduced as following, and the forward, lateral and vertical moving directions individually refer to the X, Y and Z-axis.

A. Cross a thin plane

This experiment aims to simulate a case in which the robot rolls forward while a thin plane stands on the way. Instead of making a detour, hybrid locomotion allows the robot to

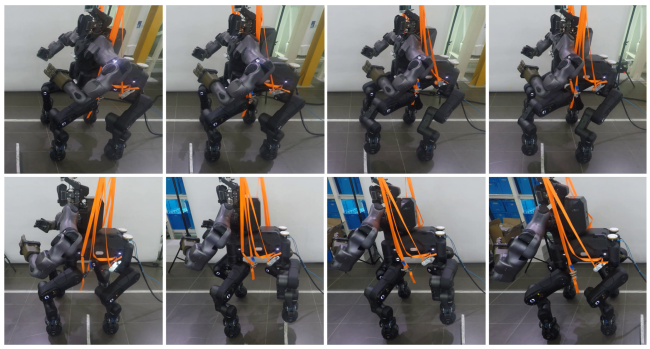

Fig. 5. Snapshots of Pholus crossing a 10cm high plane (picture interval 4s). The robot kept driving without stopping by lifting its front and hind left legs one by one and maintained the balance all the time.

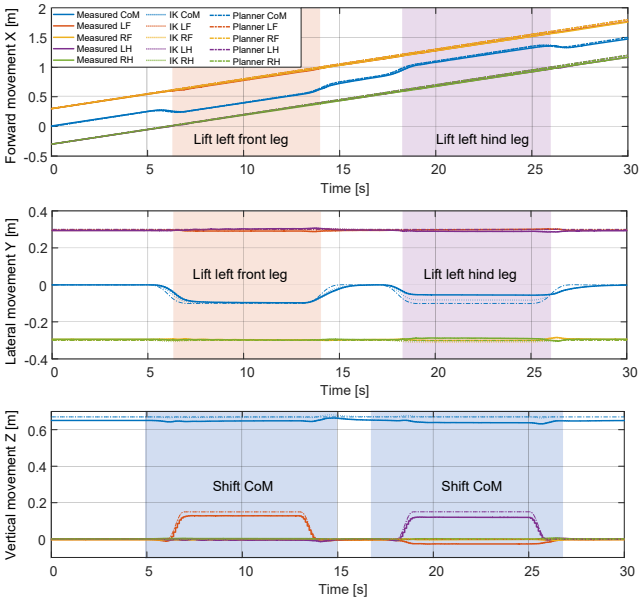

Fig. 6. Trajectories of CoM and feet when crossing a thin plane (Blue, red, yellow, purple and green lines individually indicate the CoM, LF, RF, LH and RH legs, the solid lines represent the measured data while the dot-dash lines stand for the desired ones, and the dot lines are the results solved by whole-body IK controller given the desired trajectories).

keep moving without stopping and cross the plane by lifting its legs like what animals or human usually do. Fig. 5 shows the snapshots of how the robot crossed.

In this and following experiments, one Intel RealSense Camera mounted on the chest kept detecting the pose and shape of obstacles, and desired movements were generated online at 200Hz. Here, the obstacle plane was put on the left side. Therefore, CoM was shifted to the right first before left legs were lifted up to step over. Since the robot drove across the plane continuously in hybrid mode, there was no need of switching back and forth between driving and walking modes which guarantees more efficient movement. As shown in Fig. 6, three types of trajectories of CoM and feet were recorded: desired ones generated directly from motion planner, results solved by whole-body controller and the real ones measured from encoder readings. To be noted, the whole-body controller needs to consider physical limits and do tradeoff between

Fig. 7. Snapshots of Pholus crossing long bricks (picture interval 7s). The robot stepped on the bricks, rolled and then stepped off. Meanwhile, it kept driving without stopping and maintained the balance all the way.

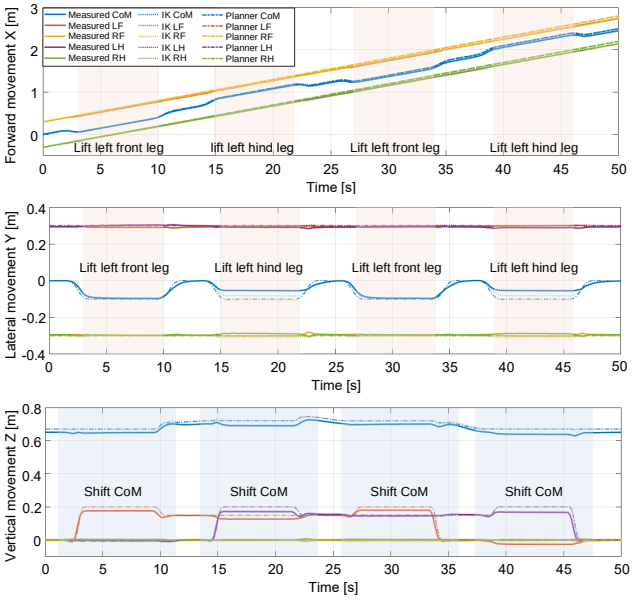

Fig. 8. Trajectories of CoM and feet when crossing long bricks (Blue, red, yellow, purple and green lines individually indicate the CoM, LF, RF, LH and RH legs, the solid lines represent the measured data while the dot-dash lines stand for the desired ones, and the dot lines are the results solved by whole-body IK controller given the desired trajectories).

different objectives which means the resulting trajectories may not be exactly the same as the planned ones. This is obvious when we look at the lateral movement of CoM. Since the driving velocity was not high, the hind left leg was allowed to lift up after the front left leg already touched on the ground. Therefore, the desired CoM movements during these two periods could be considered as identical. However, the mechanical design of this robot constrained the movement of CoM when lifting hind legs which resulted in slightly different IK solutions and real robot behaviours.

B. Cross long bricks

Similar to the first experiment, we designed another test scenario to emphasize the advantage of hybrid locomotion where some long bricks (height 15cm, total length 120cm) blocked half of the way and the robot was not allowed to make a detour. Different from stepping over the thin plane

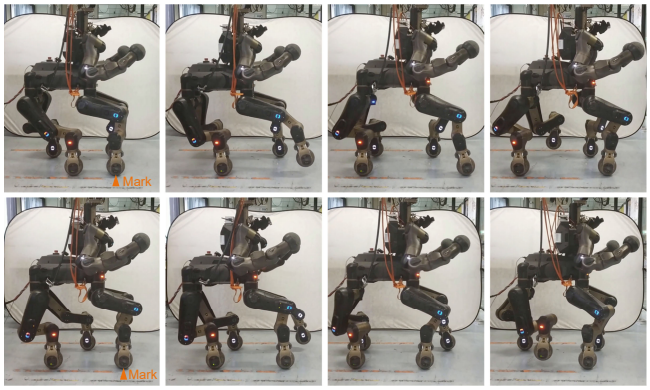

Fig. 9. Snapshots of Pholus moonwalk (picture interval 1s). The robot pretended to walk forward by swinging legs forward in sequence while actively rolling back the wheels after touching down. As indicated by the orange mark, the robot almost stayed in place without moving after the moonwalk.

aforementioned, here we expect the robot to step on the bricks and roll considering the bricks are long and strong enough to hold, which provides better motion stability. The snapshots of this experiment are shown in Fig. 7, and recorded motion trajectories are shown in Fig. 8.

Observing the data shown in Fig. 8, we can find the movements are quite similar to the previous experiment except that the whole process was extended and the left legs rolled on the obstacle instead of lifting all the time during crossing. One notable thing in this experiment is the active CoM height changing with respect to terrain variance as mentioned in Section II-B. Instead of keeping a constant CoM height, here the desired height was decided by the heights of all supporting legs. Therefore, the desired CoM height would increase when stepping on the block and decrease during stepping off.

C. Moonwalk

The stunning moonwalk show given by Michael Jackson left a deep impression to the audience. Recently, the robot Spot from Boston Dynamics demonstrated a gorgeous quadrupedal version of moonwalk. Although our robot Pholus is not as agile as human or the Spot, the equipped wheels endow the advantage of replacing the passive sliding back with actively rolling back which is usually considered as the most difficult skill in moonwalk. As shown in Fig. 9, we succeeded to implement this typical hybrid wheeled-legged locomotion skill on our robot.

The robot started from a homing posture where the four feet resting on the ground formed a rectangle with the ground projection of CoM lying at its geometric centre, and then lifted up and swung forward the legs in the order: left front $\rightarrow$ right hind $\rightarrow$ right front $\rightarrow$ left hind. After each leg touching down, the wheel installed under the foot would actively roll back to restore its original place. Within this period, different from pure driving mode or walking mode, the shape of support polygon kept changing since there was always one supporting leg rolling on the ground. The tracking data of this experiment is shown in Fig. 10.

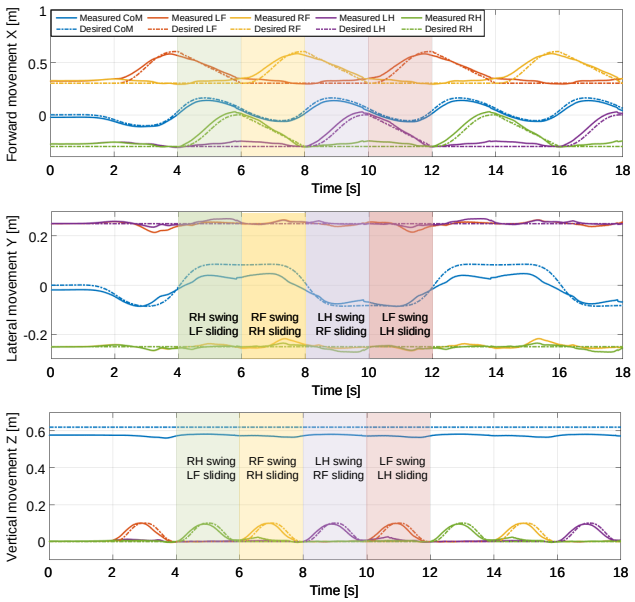

Fig. 10. Trajectories of Pholus CoM and feet during moonwalk (Blue, red, yellow, purple and green lines individually indicate the CoM, left front, right front, left hind and right hind legs, and the solid line stands for the measured data while the dash line represents the desired data).

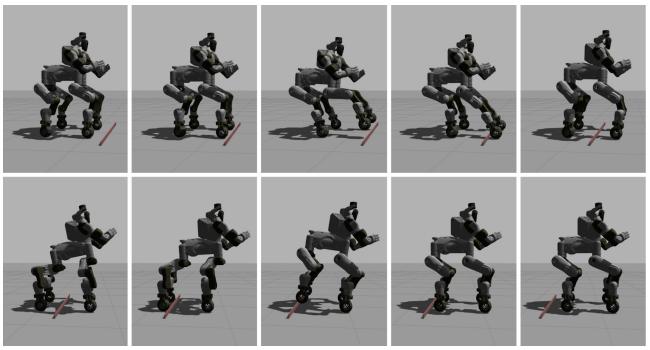

Fig. 11. Snapshots of Pholus bounding over a 5cm high plane (Picture interval 1 second). The robot shifted its CoM back and forth drastically to allow for lifting legs to cross the plane during driving.

D. Bound over a plane

To further demonstrate the capability of hybrid locomotion on more dynamic scenarios, we carried out a simulation where the robot would use a bounding-like motion to cross a thin plane. As the snapshots Fig. 11 show, Pholus was driving forward and both left and right sides were blocked by the obstacle plane. Instead of bypassing, the robot chose to lift up two front or hind legs together and kept driving at the same time. To achieve this, CoM was shifting significantly between hind legs and front legs along forward direction. Because of some hardware limitations such as maximum output torques of joint actuators and limited power supply, so far we haven't implemented this on our real robot. More details about this simulation can check the accompanying video (https://youtu.be/C6xJbMQEkqo).

V. Conclusion

In this paper, a control framework was proposed to address the hybrid locomotion problem of wheeled-legged robots. General mathematical representation of foot movement is developed to analyze different motion modes and decide hybrid foot placements. Gait graph widely used in legged locomotion is extended with extra foot velocity information to better describe the hybrid movement. Given the planned foot placements, MPC is implemented to optimize the CoM trajectory considering terrain height changing. Desired trajectories together with other kinematic and dynamic constraints are fed into a whole-body controller, a quadratic-programming solver, to produce joint commands. In the end, the feasibility of the proposed approach is demonstrated by several successful hybrid locomotion simulation and experiments running on our wheeled quadrupedal robot Pholus.

Future research will be carried out in two aspects. First, the foot placement planning can be more intelligent by utilizing deep reinforcement learning to determine motion modes and velocities. On the other side, the whole-body control can be further improved on the tracking accuracy and movement stability by considering more dynamics given the joint torque control capability of our Pholus robot.

References

[1] M. Raibert, K. Blankespoor, G. Nelson, and R. Playter, "Bigdog, the rough-terrain quadruped robot," *IFAC Proceedings Volumes*, vol. 41, no. 2, pp. 10 822–10 825, 2008.

[2] S. Claudio, "Hyq-design and development of a hydraulically actuated quadruped robot," *Liguria, Italy, University of Genoa*, pp. 10–15, 2010.

[3] W. Bosworth, S. Kim, and N. Hogan, "The MIT super mini cheetah: A small, low-cost quadrupedal robot for dynamic locomotion," in *Proc. and Rescue Robotics (SSRR) 2015 IEEE Int. Symp. Safety, Security*, Oct. 2015, pp. 1–8.

[4] A. W. Winkler, F. Farshidian, M. Neunert, D. Pardo, and J. Buchli, "Online walking motion and foothold optimization for quadruped locomotion," in *2017 IEEE International Conference on Robotics and Automation (ICRA)*. IEEE, 2017, pp. 5308–5313.

[5] N. Kashiri, L. Baccelliere, L. Muratore, A. Laurenzi, Z. Ren, E. M. Hoffman, M. Kamedula, G. F. Rigano, J. Malzahn, S. Cordasco, P. Guria, A. Margan, and N. G. Tsagarakis, "Centauro: A hybrid locomotion and high power resilient manipulation platform," *IEEE Robotics and Automation Letters*, vol. 4, no. 2, pp. 1595–1602, Apr. 2019.

[6] B. d'Andréa Novel, G. Campion, and G. Bastin, "Control of nonholonomic wheeled mobile robots by state feedback linearization," *The International journal of robotics research*, vol. 14, no. 6, pp. 543–559, 1995.

[7] G. Artus, P. Morin, and C. Samson, "Control of a maneuvering mobile robot by transverse functions," in *On Advances in Robot Kinematics*. Springer, 2004, pp. 459–468.

[8] C. Hubicki, J. Grimes, M. Jones, D. Renjewski, A. Spröwitz, A. Abate, and J. Hurst, "Atrias: Design and validation of a tether-free 3d-capable spring-mass bipedal robot," *The International Journal of Robotics Research*, vol. 35, no. 12, pp. 1497–1521, 2016.

[9] G. Endo, J. Morimoto, T. Matsubara, J. Nakanishi, and G. Cheng, "Learning cpg-based biped locomotion with a policy gradient method: Application to a humanoid robot," *The International Journal of Robotics Research*, vol. 27, no. 2, pp. 213–228, 2008.

[10] M. Neunert, M. Stäuble, M. Giftthaler, C. D. Bellicoso, J. Carius, C. Gehring, M. Hutter, and J. Buchli, "Whole-body nonlinear model predictive control through contacts for quadrupeds," *arXiv preprint arXiv:1712.02889*, 2017.

[11] A. Laurenzi, E. M. Hoffman, and N. G. Tsagarakis, "Quadrupedal walking motion and footstep placement through linear model predictive control," in *2018 IEEE/RSJ International Conference on Intelligent Robots and Systems (IROS)*. IEEE, 2018, pp. 2267–2273.

[12] M. Kamedula, N. Kashiri, and N. G. Tsagarakis, "On the kinematics of wheeled motion control of a hybrid wheeled-legged centauro robot," in *2018 IEEE/RSJ International Conference on Intelligent Robots and Systems (IROS)*. IEEE, 2018, pp. 2426–2433.

[13] K. Nagano and Y. Fujimoto, "The stable wheeled locomotion in low speed region for a wheel-legged mobile robot," in *2015 IEEE International Conference on Mechatronics (ICM)*. IEEE, 2015, pp. 404–409.

[14] A. Dietrich, K. Bussmann, F. Petit, P. Kotyczka, C. Ott, B. Lohmann, and A. Albu-Schäffer, "Whole-body impedance control of wheeled mobile manipulators," *Autonomous Robots*, vol. 40, no. 3, pp. 505–517, 2016.

[15] A. Dietrich, T. Wimböck, and A. Albu-Schäffer, "Dynamic whole-body mobile manipulation with a torque controlled humanoid robot via impedance control laws," in *2011 IEEE/RSJ International Conference on Intelligent Robots and Systems*. IEEE, 2011, pp. 3199–3206.

[16] J. Lim, I. Lee, I. Shim, H. Jung, H. M. Joe, H. Bae, O. Sim, J. Oh, T. Jung, S. Shin *et al.*, "Robot system of drc-hubo+ and control strategy of team kaist in darpa robotics challenge finals," *Journal of Field Robotics*, vol. 34, no. 4, pp. 802–829, 2017.

[17] P. Hebert, M. Bajracharya, J. Ma, N. Hudson, A. Aydemir, J. Reid, C. Bergh, J. Borders, M. Frost, M. Hagman *et al.*, "Mobile manipulation and mobility as manipulationdesign and algorithms of robosimian," *Journal of Field Robotics*, vol. 32, no. 2, pp. 255–274, 2015.

[18] M. Schwarz, T. Rodehutskors, M. Schreiber, and S. Behnke, "Hybrid driving-stepping locomotion with the wheeled-legged robot momaro," in *2016 IEEE International Conference on Robotics and Automation (ICRA)*. IEEE, 2016, pp. 5589–5595.

[19] T. Klamt and S. Behnke, "Anytime hybrid driving-stepping locomotion planning," in *Proc. IEEE/RSJ Int. Conf. Intelligent Robots and Systems (IROS)*, Sep. 2017, pp. 4444–4451.

[20] T. Klamt, D. Rodriguez, M. Schwarz, C. Lenz, D. Pavlichenko, D. Droeschel, and S. Behnke, "Supervised autonomous locomotion and manipulation for disaster response with a centaur-like robot," in *2018 IEEE/RSJ International Conference on Intelligent Robots and Systems (IROS)*. IEEE, 2018, pp. 1–8.

[21] Y. de Viragh, M. Bjelonic, C. D. Bellicoso, F. Jenelten, and M. Hutter, "Trajectory optimization for wheeled-legged quadrupedal robots using linearized zmp constraints," *IEEE Robotics and Automation Letters*, 2019.

[22] M. Bjelonic, C. D. Bellicoso, Y. de Viragh, D. Sako, F. D. Tresoldi, F. Jenelten, and M. Hutter, "Keep rollin'-whole-body motion control and planning for wheeled quadrupedal robots," *IEEE Robotics and Automation Letters*, 2019.

[23] M. Geilinger, R. Poranne, R. Desai, B. Thomaszewski, and S. Coros, "Skaterbots: Optimization-based design and motion synthesis for robotic creatures with legs and wheels," *ACM Transactions on Graphics (TOG)*, vol. 37, no. 4, p. 160, 2018.

[24] M. Schwarz, T. Rodehutskors, M. Schreiber, and S. Behnke, "Hybrid driving-stepping locomotion with the wheeled-legged robot momaro," in *Proc. IEEE Int. Conf. Robotics and Automation (ICRA)*, May 2016, pp. 5589–5595.

[25] A. Herdt, H. Diedam, P.-B. Wieber, D. Dimitrov, K. Mombaur, and M. Diehl, "Online walking motion generation with automatic footstep placement," *Advanced Robotics*, pp. 719–737, 2010.

[26] D. E. Orin, A. Goswami, and S.-H. Lee, "Centroidal dynamics of a humanoid robot," *Autonomous Robots*, vol. 35, no. 2-3, pp. 161–176, 2013.

[27] L. Sentis and O. Khatib, "A whole-body control framework for humanoids operating in human environments," in *Proc. IEEE Int. Conf. Robotics and Automation ICRA 2006*, May 2006, pp. 2641–2648.

[28] M. Hutter, H. Sommer, C. Gehring, M. Hoepflinger, M. Bloesch, and R. Siegwart, "Quadrupedal locomotion using hierarchical operational space control," *The International Journal of Robotics Research*, 2014.

[29] A. Escande, N. Mansard, and P.-B. Wieber, "Hierarchical quadratic programming: Fast online humanoid-robot motion generation," *The International Journal of Robotics Research*, vol. 33, no. 7, pp. 1006–1028, 2014.

[30] A. Herzog, L. Righetti, F. Grimminger, P. Pastor, and S. Schaal, "Balancing experiments on a torque-controlled humanoid with hierarchical inverse dynamics," in *Proc. IEEE/RSJ Int. Conf. Intelligent Robots and Systems*, Sep. 2014, pp. 981–988.

[31] E. M. Hoffman, A. Rocchi, A. Laurenzi, and N. G. Tsagarakis, "Robot control for dummies: Insights and examples using opensot," in *Proc. IEEE-RAS 17th Int. Conf. Humanoid Robotics (Humanoids)*, Nov. 2017, pp. 736–741.